European Journal of Pharmaceutics and Biopharmaceutics 179 (2022) 47–57

Contents lists available at ScienceDirect

European Journal of Pharmaceutics and Biopharmaceutics

journal homepage: www.elsevier.com/locate/ejpb

Elucidation of lactose fine size and drug shape on rheological properties and aerodynamic behavior of dry powders for inhalation

Ying Sun [a], Duo Yu [a], Jiayi Li [a], Jianan Zhao [b], Yu Feng [b], Xin Zhang [a], Shirui Mao [a,*]

[a] School of Pharmacy, Shenyang Pharmaceutical University, Shenyang 110016, China
[b] School of Chemical Engineering, Oklahoma State University, Stillwater 74074, USA

ARTICLE INFO

Keywords:
Dry powder inhaler (DPI)
Optimum fines size and shape
Computational fluid dynamics
Lung deposition prediction

ABSTRACT

Pulmonary drug delivery has gained great attention in local or systemic diseases therapy, however it is still difficult to scale-up DPI production due to the complexity of interactions taking place in DPI systems and limited understanding between flowability and inter-particle interactions in DPI formulations. Therefore, finding some quantitative parameters related to DPI delivery performance for predicting the *in vitro* drug deposition behavior is essential. Therefore, this study introduces a potential model for predicting aerodynamic performance of carrier-based DPIs, as well to find more relevant fine powder size and optimal shape to improve aerodynamic performance. Using salbutamol sulfate as a model drug, Lactohale®206 as coarse carrier, Lactohale®300, Lactohale®230, and Lactohale®210 as third fine components individually, the mixtures were prepared at 1% (w/w) drug content accompanied with carriers and the third component (ranging from 3% to 7%), influence of lactose fines size on DPI formulation's rheological and aerodynamic properties was investigated. The optimum drug particle shape was also confirmed by computer fluid dynamics model. This study proved that pulmonary deposition efficiency could be improved by decreasing lactose fines size. Only fines in the size range of 0–11 μm have a good linear relationship with FPF, attributed to the fluidization energy enhancement and aggregates mechanism. Once exceeding 11 μm, fine lactose would act as a second carrier, with increased drug adhesion. Computational fluid dynamics (CFD) models indicated fibrous drug particles were beneficial to transfer to the deep lung. Furthermore, good correlations between rheological parameters and FPF of ternary mixtures with different lactose fines were established, and it was disclosed that the FPF was more dependent on interaction parameters than that of flowability.

1. Introduction

Pulmonary drug delivery has attracted a lot of interests in recent decades because of its rapid onset of action to treat local airway diseases, such as asthma or COPD, as well as to offer a great potential to treat systemic diseases such as diabetes, migraines and cancer pain or immunization [1]. Among the commonly used pulmonary dosage forms, DPIs have good user accessibility and excellent performance. DPI formulations on the market are mainly composed of respirable drug particles (micronized, aerodynamic diameter 1–5 μm) mixed with carriers (diameter 50–200 μm) [2], and more than three-quarters of the commercially available DPIs use lactose as a carrier [3]. Other carriers such as mannitol, sucrose, trehalose, and sorbitol can also be used as candidates for patients with lactose intolerance [4], However, so far only lactose and mannitol (approved in Exubera® /Bronchitol®) are approved by FDA for pulmonary application, others are scientifically under investigation. Moreover, in order to improve lung deposition, additional fine excipients are often used to reduce the surface energy

Abbreviations: DPI, dry powder inhaler; CFD, computational fluid dynamics; FPF, fine particle fraction; COPD, chronic obstructive pulmonary disease; SMI, soft mist inhaler; MDI, metered-dose inhaler; BFE, basic flowability energy; AE, aeration energy; AR, aeration ratio; PCA, principal component analysis; SS, salbutamol sulfate; LH206, Lactohale®206; LH300, Lactohale®300; LH230, Lactohale®230; LH210, Lactohale®210; RSD, relative standard deviation; PSD, particle size distribution; SEM, scanning electron microscopy; FF, flowability function; NGI, Next Generation Impactor; EF, emitted fraction; MMAD, mass median aerodynamic diameter; D10, volumetric diameter value at 10% of cumulative distribution; D50, volumetric diameter value at 50% of cumulative distribution; D90, volumetric diameter value at 90 % of cumulative distribution; DFs, regional deposition fractions; LLL, left lower lobe; LUL, left upper lobe; RLL, right lower lobe; RML, right middle lobe; RUL, right upper lobe; MT, mouth-to-throat region; PC (1;2), principal component (1;2); TCS, total component score.

* Corresponding author at: School of Pharmacy, Shenyang Pharmaceutical University, 103 Wenhua Road, Shenyang 110016, China.
E-mail address: maoshirui@syphu.edu.cn (S. Mao).

https://doi.org/10.1016/j.ejpb.2022.08.007
Received 19 May 2022; Received in revised form 17 August 2022; Accepted 19 August 2022
Available online 25 August 2022

Table 1
Particle size distribution and blend uniformity of different samples used in this study (n = 3).

Material	D10 (μm)	D50 (μm)	D90 (μm)	Particles <5 μm (%)	Recovery Rate (%)	RSD (%)
SS	0.58 ± 0.03	1.97 ± 0.04	5.03 ± 0.10	89.92 ± 0.54	_	_
LH300	0.61 ± 0.01	2.86 ± 0.02	7.39 ± 0.22	75.44 ± 0.61	_	_
LH230	1.29 ± 0.06	7.46 ± 0.19	19.87 ± 1.38	35.68 ± 0.73	_	_
LH210	3.00 ± 0.02	14.42 ± 0.08	35.09 ± 0.20	19.81 ± 0.18	_	_
LH206	28.43 ± 0.45	79.59 ± 0.65	156.22 ± 0.07	2.56 ± 0.10	_	_
99 % LH206-1 %SS	24.56 ± 0.74 *	78.15 ± 0.73	153.86 ± 1.58	3.82 ± 0.15*	92.68 ± 1.96	2.12
3 % LH300-96 % LH206-1 %SS	10.62 ± 0.10 *	74.75 ± 0.12 *	154.45 ± 1.15	7.06 ± 0.05 *	95.58 ± 3.54	3.71
5 % LH300-94 % LH206-1 %SS	5.88 ± 0.03 *	71.84 ± 0.27 *	152.95 ± 1.55*	9.61 ± 0.03*	94.35 ± 2.23	2.36
7 % LH300-92 % LH206-1 %SS	4.42 ± 0.05 *	70.31 ± 0.64 *	151.23 ± 0.75*	11.74 ± 0.16 *	94.24 ± 1.18	1.25
3 % LH230-96 % LH206-1 %SS	19.02 ± 0.24 *	77.75 ± 0.09 *	147.91 ± 1.77*	4.84 ± 0.01*	95.02 ± 1.48	1.55
5 % LH230-94 % LH206-1 %SS	12.08 ± 0.24 *	75.34 ± 0.56 *	146.51 ± 1.25*	5.78 ± 0.05 *	99.82 ± 3.81	3.81
7 % LH230-92 % LH206-1 %SS	9.10 ± 0.10 *	73.61 ± 0.23 *	147.75 ± 0.61*	6.74 ± 0.04 *	97.37 ± 0.93	0.95
3 % LH210-96 % LH206-1 %SS	23.35 ± 0.23 *	78.48 ± 0.60	147.84 ± 2.76*	4.13 ± 0.02*	95.36 ± 3.03	3.18
5 % LH210-94 % LH206-1 %SS	18.46 ± 0.48 *	76.56 ± 0.27 *	147.80 ± 0.32*	4.60 ± 0.11 *	95.69 ± 1.72	1.80
7 % LH210-92 % LH206-1 %SS	15.27 ± 0.34 *	74.90 ± 0.29 *	146.20 ± 0.56*	4.91 ± 0.08 *	97.14 ± 1.09	1.13

* $p < 0.05$, compared to LH206 group.

among particles by yielding a higher surface coverage, such as magnesium stearate, or creating more rough surface by reducing interparticulate contact area, such as L-leucine [5]. Lactose fines is commonly used in carrier based DPI formulations. Other substances, such as leucine [6], albumin and phosphatidylcholine [7], are also employed in engineered particles, they could migrate to the particle surface during spray drying, improving dispersion behavior and preventing moisture absorption. Once such inhaled particles deposited in the lung, they would dissolve gradually. However, mucociliary clearance and macrophage phagocytosis in the lung microenvironment may decrease drug absorption [8]. In addition, surface characteristics of the particle, such as hydrophobicity and surface charge, can also influence its retention in the lung [9].

The composition of carrier based DPI formulations may seem simple, however, to achieve required lung deposition, an ideal adhesive mixture should be homogeneous and stable, and can be easily separated into single particles upon aerosolization, that is, force balance during mixing and aerosolization process should be maintained. On one hand, the strong drug-carrier adhesion force is beneficial for the formation of stable mixture during mixing and filling, with required stability during shelf life. On the other hand, since only free particles can be delivered deep into the lung, the force between drug and carrier particles should not be too strong so as to be separated by the dispersion forces generated in DPI device [10]. In general, the dispersion forces involved in DPI devices include lift and drag forces, friction and shear forces (e.g. Cyclohaler®), as well inertial forces (e.g. Novolizer®) [2]. Although a great effort has been made to increase the total lung deposition from <10% to between 20% and 40% for currently marketed carrier-based formulations, still less than half of the dose can be delivered to the site of action because of the high cohesiveness of the fine drug powders [11].

Numerous studies have demonstrated that the presence of fine excipient particles can improve *in vitro* lung deposition performance of DPIs based on several theories, such as the “active site” mechanism suggesting fine particles compete with drug particles at high energy site [12–14], agglomeration mechanism suggesting large aggregates of fine excipient and micronized drug particles are subject to stronger aerodynamic drag forces [14–16], fluidization enhancement mechanism suggesting fine particles strengthen aerodynamic dispersion forces [14,17], buffer mechanism suggesting fine particles protect drug particles from suffering the mixing pressure [18], and fine particle network mechanism suggesting fines with a slightly larger size can prevent the network structure formation on carrier surface whereas the drug particles might be trapped [19,20]. These five hypothesis are beneficial, however the press-on mechanism reveals a negative influence. The negative influence is proposed when more fine particles occupy irregularities on the carrier surface, which exhibits increased susceptibility to compressive mixing process [19]. Our previous study [21] also shows the *in vitro* deposition performance is mediated by interplay of several mechanisms depending on the fine content. Moreover, some studies have indicated that the fines size is also an important factor influencing DPI performance [22,23]. However, the influence of fines size on the flow, fluidization and dispersion behavior of the ternary mixtures is still unclear, it is also unknown whether these powder characteristics can be used for *in vitro* lung deposition prediction.

Since the performance of adhesive mixtures is manipulated by both drug inter-particulate and drug-carrier interactions, a single (independently) particle property cannot predict overall behavior of DPI powders. Given the inhalation process of DPI powders, a potential way to predict *in vitro* performance should closely relate to real inhalation process. Thus, powder rheology can be a good choice with air introduction during testing, simulating the fluidization, dispersion and aerosolization process when DPI powders are delivered to the body via device [24], which provides a potential to improve the reliability and accuracy of *in vitro* prediction.

Thus, the objective of this study was to investigate the influence of extrinsic fine lactose size on the *in vitro* drug deposition based on DPI’s rheological properties. The influence of fine lactose size on powder’s flow, fluidization and aerosolization behavior was explored explicitly based on the flowability parameter and interaction parameters, and the influence of drug particle shape was predicted via computer fluid dynamics model. Finally, principal component analysis (PCA) was used to describe the dependence of FPF on powder properties.

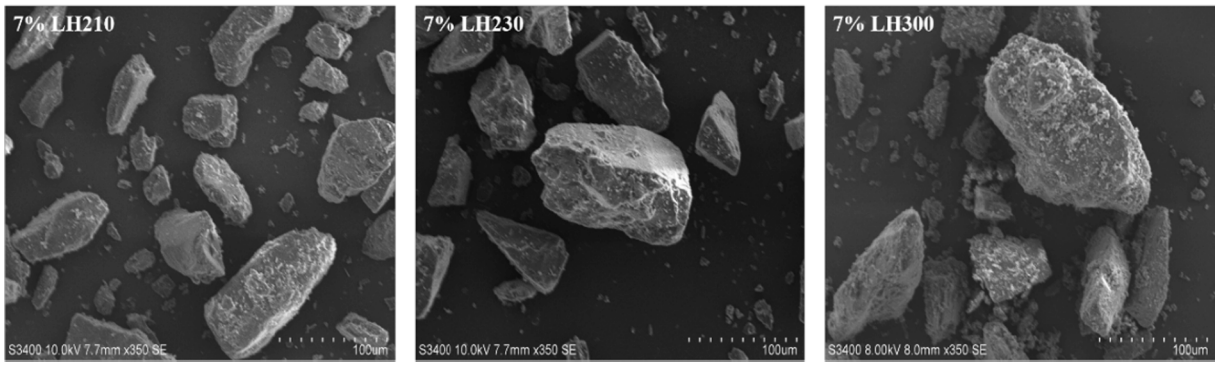

Fig. 1. Morphology of the ternary physical mixtures (SS + carrier + fines) visualized with SEM. Images taken at 350× magnification.

Table 2
Rheological characteristics of the carriers and DPI powders (n = 3).

Material	BFE(mJ)	AE(mJ)	AR	Permeability (10^-9 cm^2)	FF	Cohesion (kPa)
LH206	566.67 ± 8.74	47.77 ± 2.11	9.95 ± 0.97	43.27 ± 2.92	10.91 ± 1.19	0.390 ± 0.049
3 %LH300-96 %LH206-1 %SS	302.33 ± 8.08#	46.37 ± 2.83	7.77 ± 0.67#	19.17 ± 0.03#	7.10 ± 0.23#	0.612 ± 0.026#
3 %LH230-96 %LH206-1 %SS	372.00 ± 12.17#	42.40 ± 4.68	9.06 ± 0.80	29.14 ± 0.36#	9.26 ± 1.20	0.461 ± 0.061
3 %LH210-96 %LH206-1 %SS	374.00 ± 7.81#	39.60 ± 1.08#	9.86 ± 0.25	32.62 ± 1.86#	13.20 ± 1.87	0.386 ± 0.070
5 %LH300-94 %LH206-1 %SS	257.67 ± 6.11#	47.77 ± 3.00	6.84 ± 0.88#	14.62 ± 0.65#	6.46 ± 0.81#	0.677 ± 0.095#
5 %LH230-94 %LH206-1 %SS	342.00 ± 7.21#	46.33 ± 2.94	8.71 ± 0.45	23.75 ± 0.59#	8.75 ± 0.73	0.484 ± 0.046
5 %LH210-94 %LH206-1 %SS	364.33 ± 9.29#	39.10 ± 2.26#	9.75 ± 0.34	28.11 ± 0.88#	9.57 ± 0.94	0.446 ± 0.047
7 %LH300-92 %LH206-1 %SS	234.00 ± 4.58#	51.70 ± 4.60	5.78 ± 0.42#	11.23 ± 0.20#	5.64 ± 0.29#	0.765 ± 0.045#
7 %LH230-92 %LH206-1 %SS	308.33 ± 2.31#	51.37 ± 1.91	7.29 ± 0.34#	19.71 ± 0.46#	7.14 ± 0.84#	0.607 ± 0.077#
7 %LH210-92 %LH206-1 %SS	348.67 ± 13.61#	42.17 ± 2.30#	9.08 ± 0.62	24.87 ± 0.20#	8.32 ± 0.58#	0.517 ± 0.041#

# $p < 0.05$, compared to LH206 group.

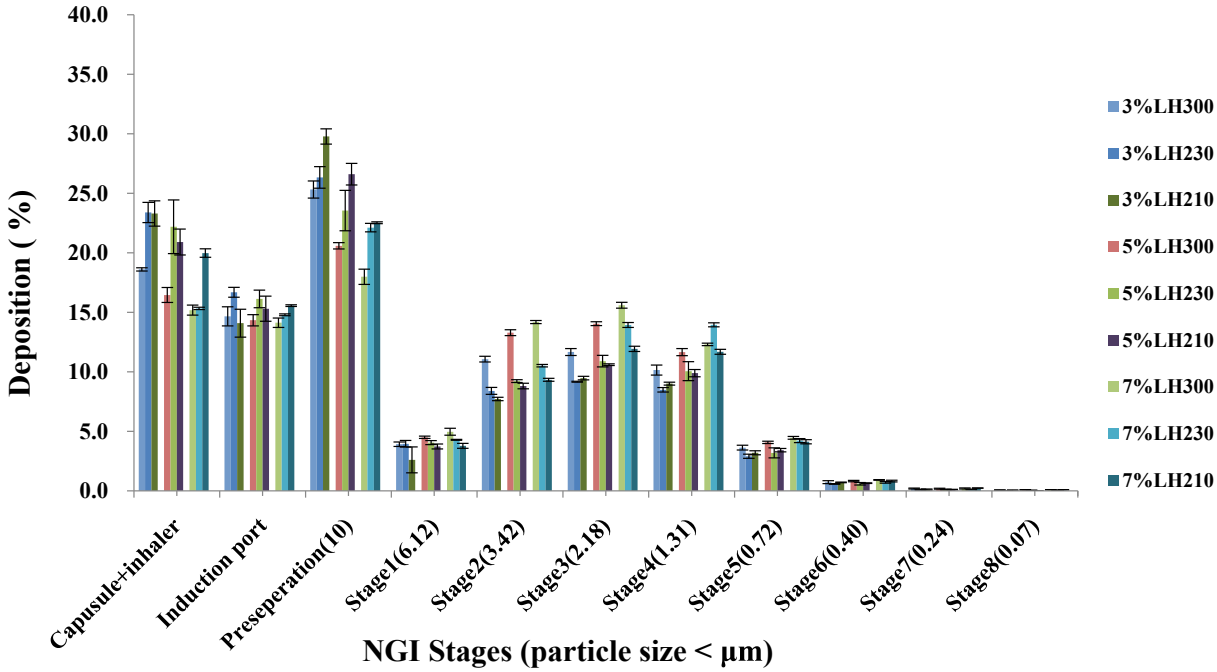

Fig. 2. Aerodynamic particle size distribution of all the mixtures by NGI (n = 3).

2. Materials and methods

2.1. Materials

Salbutamol sulphate (SS) was purchased from Xiya Reagent Pharmaceutical Ltd (China). Lactohale® 206 (LH206) Lactohale® 300, 230, 210 (LH300, LH230, LH210) were donated by DFE Pharma (China). All other materials were of analytical grade unless otherwise specified.

2.2. Formulations preparation and characterization

The method used to prepare and characterize DPI formulations was described as reported previously [25]. Briefly, micronized SS, carriers and fines were sieved to break up large aggregates and subsequently

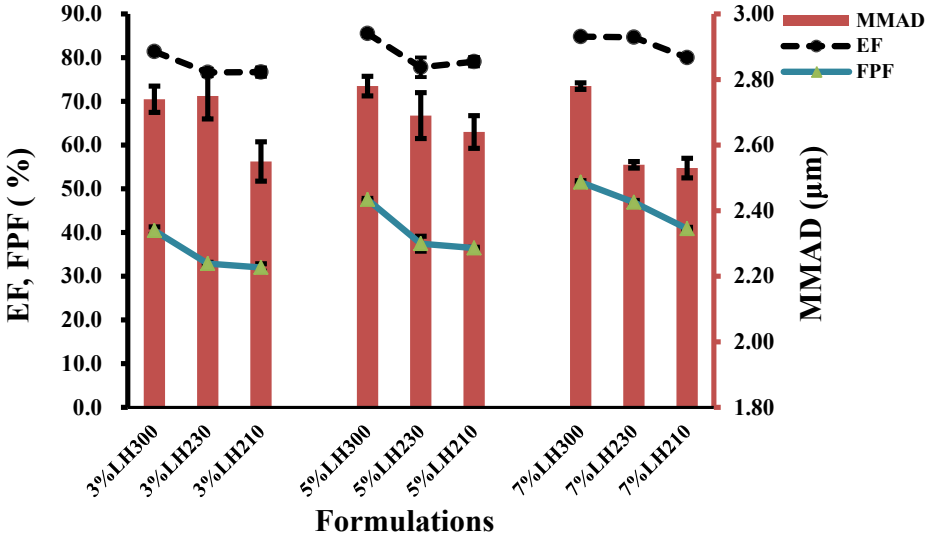

Fig. 3. Aerodynamic performances (MMAD, EF, and FPF) of all the DPI mixtures measured by NGI (n = 3).

placed in a manipulatable environment (20 ± 2 °C and 45 ± 5% RH) overnight. The blending process contained two steps. Firstly, the fine lactose and carriers were mixed manually to form premixtures, then drug particles were blended with such premixtures in a sandwich manner (premixtures-drugs-premixtures) with Mini-G mixer (Xin Yi Te Technology Co., Ltd. China) in the second blending step for 5 min (at 100 rpm speed) and another 4 min (at 300 rpm). In total, 180 g mixtures were prepared at 1% (w/w) drug content accompanied with different fine sizes and content (ranging from 3% to 7%). RSD of drug recovery rate can be used to describe blend uniformity, which can be calculated based on the following Eq. (1):

$$\text{Recovery rate} = (\text{measured drug content} / \text{theoretical drug content}) \times 100\ \% \quad (1)$$

Whereas, the drug content was measured with UV spectroscopy method at 276 nm using distilled water as the medium (Unico, Shanghai).

Particle size distribution (PSD) was determined with laser light diffraction technique (HELOS/KR, Sympatec GmbH, Germany). A dry dispersing system (Rodos module) was used for powder dispersion with 4 bar pressure. R1 lens was used for drugs and fine lactose, and R5 lens was used for coarse carriers and mixtures. Cumulative volume-based particle size distribution plots were analyzed.

2.3. Morphology characterization

Scanning electron microscopy (SEM) was used to characterize morphology of DPI powders. 30 mg samples were sprinkled on an aluminum specimen and then coated with gold, finally visualized with Hitachi S-3400 (Hitachi, Japan).

2.4. Powder rheological properties characterization

FT4 rheometer (Freeman Technology, UK) was used to characterize DPI powders rheological properties as reported previously [25].

In dynamic measurement module, the tested powders were filled into a vessel with an oar moved down the axis, the recorded flow resistance during powders displacement was described as basic flowability energy (BFE). Another tested powders were put into another vessel, the operation is similar to that of the dynamic module but with additional air flow from the bottom. The energy required to make the powder flow at 0, 1, 2, 4, 6, 8, 10 mm/s air velocity is defined as flow energy, the recorded constant energy until such powders being fluidized (almost at 10 mm/s) completely is defined as aeration energy (AE). Moreover, aeration ratio (AR) is derived based on the following Eq. (2):

$$\text{AR} = (\text{Energy at 0 mm/s of air flow rate}) / (\text{aeration energy (AE)}) \quad (2)$$

In bulk measurement module, the tested powders were filled into a vessel, 2 mm/s airflow was introduced and vertical pressure was applied, then the permeability between the top and bottom was obtained.

In shear cell measurement module, the tested powders were placed into a customized vessel with pre-defined vertical stress applied, and the related cohesion parameters and flowability function (FF) were obtained from Mohr circle.

2.5. Aerodynamic properties characterization

Next Generation Impactor (NGI, Copley Scientific, UK) was used to measure aerodynamic properties of DPI powders with Cyclohaler® device at 100 L/min. 25 mg mixtures were filled into 3# Vcaps® (Capsugel®, China), 7 capsules were operated in one run during measurement. The deposited drug particles were collected and subsequently analyzed with HPLC as reported previously [21]. Three aerodynamic performance parameters were determined, including fine particle fraction (FPF), emitted fraction (EF) and mass median aerodynamic diameter (MMAD) [26]. Emitted dose (ED) is defined as the drug emitted from inhaler device, the corresponding EF is defined as the ratio of emitted dose to the recovered dose. FPF is the ratio of drug deposited at Stage 1–5 to the recovered dose. MMAD is the diameter at which 50% of the aerosol mass is larger than it.

2.6. Computational fluid dynamics modeling

Computational fluid dynamics (CFD) has been widely applied in early stages of inhalation therapy or device development process in advance of, and to complement, clinical trials. Accordingly, a CFD-based airway model here was employed to explore the influence of inhaled drug shape on the distribution of lung deposition. The one-way coupled Euler-Lagrange model was used to simulate transport dynamics of inhaled air-particle flow for spherical and non-spherical particles in human respiratory systems [27–30]. The 3-dimensional human respiratory geometry contains a representative tract from oral cavity and nasal cavity to generation 13 (G13) (Fig. 5(a)) [31,32]. A detailed description of the CFD can be found in publications [31,32].With an inhalation flow rate Q_{in} = 100 L/min, fine particles with two different shapes were simulated. Specifically, with same drug particle size

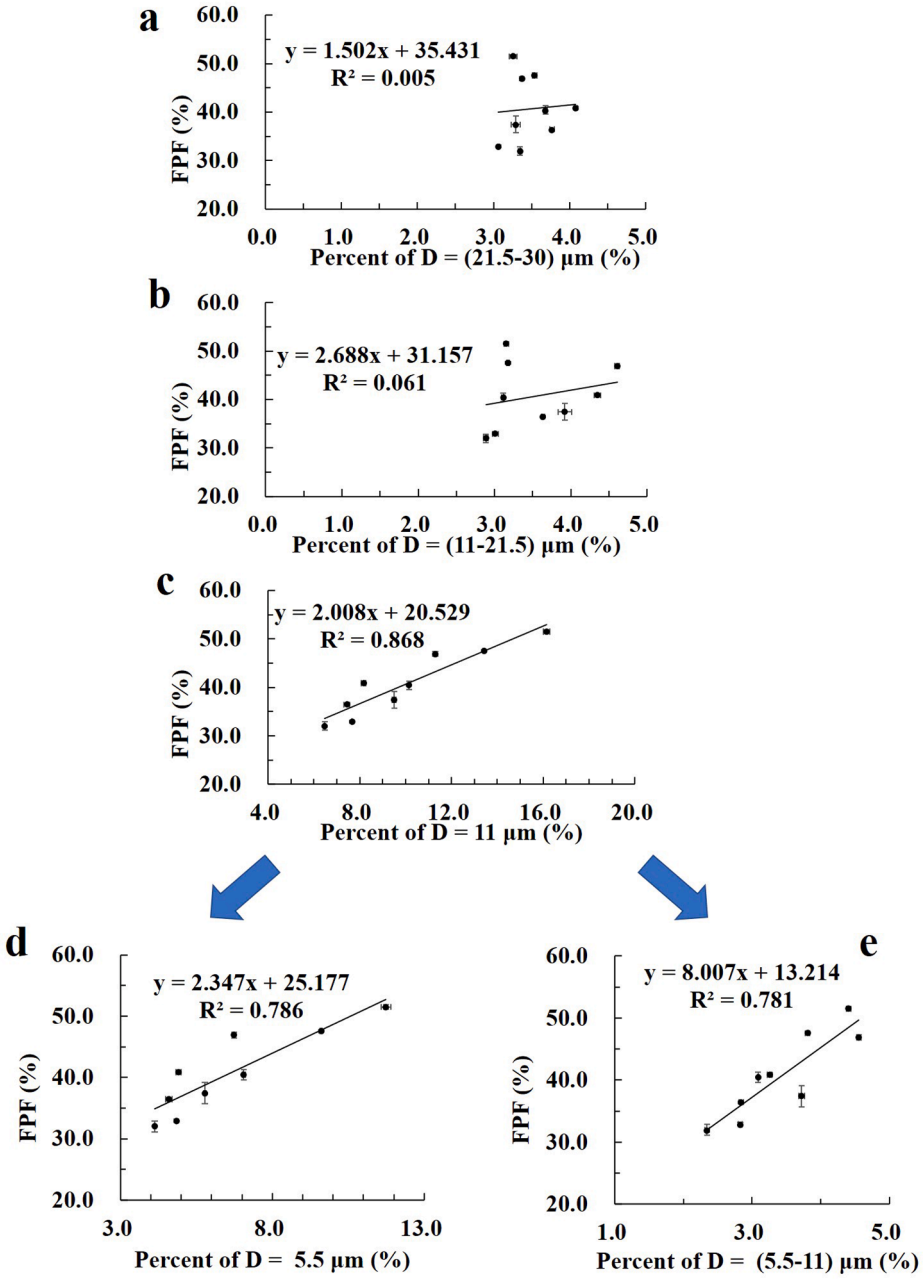

Fig. 4. Correlations between percent of fines with different size and FPF (n = 3).(a) Percent of $D_{=21.5\text{-}30\ \mu m}$ – FPF, (b) Percent of $D_{=11\text{-}21.5\ \mu m}$ – FPF, (c)Percent of $D_{=0\text{-}11\ \mu m}$ - FPF, (d) Percent of $D_{=0\text{-}5.5\ \mu m}$ – FPF, (e) Percent of $D_{=(5.5\text{-}11)\ \mu m}$ - FPF.

distributions obtained from in-house experimental study, spherical particles and elongated particles with an aspect ratio AR = 7.5 were employed to quantify the particle shape effect on particle deposition distribution (Fig. 5(b)) in human lung. CFD simulations of pulmonary air-particle flow dynamics were performed using Ansys Fluent 2021 R1 (Ansys Inc., Canonsburg, PA) on a local Dell Precision T7810 workstation (Intel® Xeon® Processor E5-2643 v4 with dual processors, 64 cores and 128 GB RAM). The semi-implicit method for pressure-linked equations (SIMPLE) algorithm was employed for the pressure–velocity coupling, and the least-squares cell-based scheme was applied to calculate the cell gradients. The second-order scheme was employed for pressure discretization.

2.7. Statistical analysis

Experimental value for statistical analysis was expressed as mean ± standard deviation (SD) with n = 3 unless otherwise specified. Two-tail *t*-test comparison with probability values $p < 0.05$ was considered to be statistically significant.

3. Results and discussion

3.1. Influence of fine lactose size on particle size and uniformity

It has been demonstrated that adding a third component can be a good strategy to improve pulmonary drug delivery [21]. However, the influence of fine lactose size on particle size and uniformity of ternary mixtures is still unclear. Therefore, in this study, a model drug (salbutamol sulfate) with inhalable particle size range (<5 μm) was mixed with coarse lactose (LH206) (about 80 μm), and three types of fine lactose powder with different size was incorporated as a third additive. The detailed particle size information is presented in Table 1, the

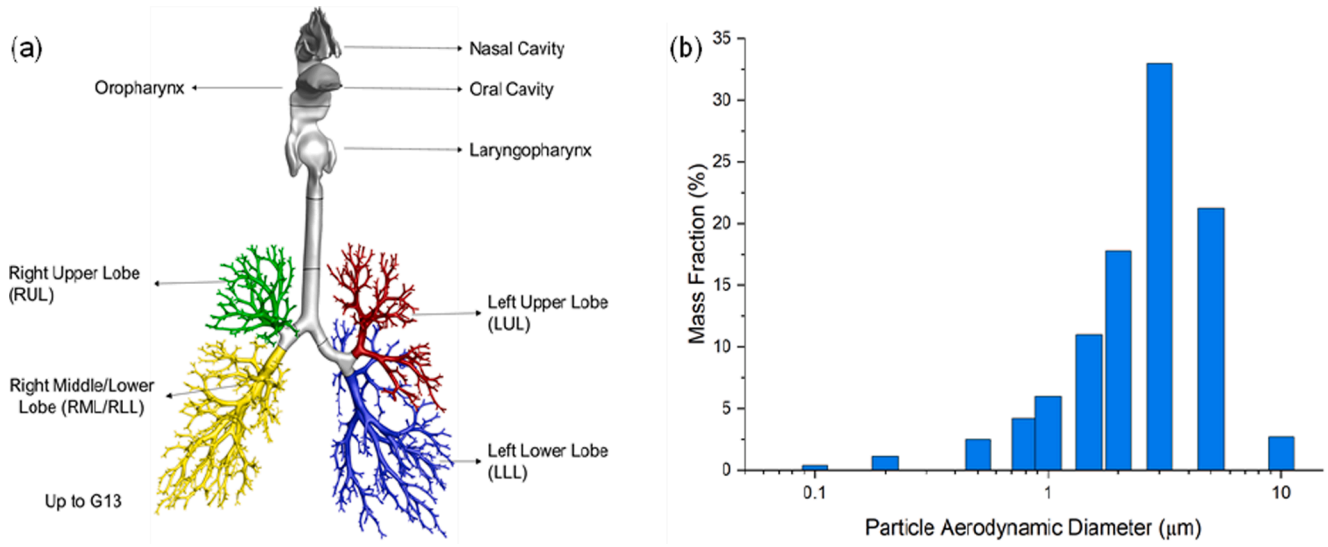

Fig. 5. (a) The 3D human respiratory tract geometry, and (b) Orally inhaled drug particle size distribution.

average size of lactose fines is ranked in the order LH300 < LH230 < LH210. It was noted that D10 and D50 of DPI powders decreased with the decrease of lactose fines size. However, the mixtures containing the smallest size lactose fine (LH300) showed a larger D90. Probably such smaller size, like LH300, were prone to attach to the carriers surface, thereby forming a larger particle aggregate [15]. Taking mixture containing 7% fines of different size as example, morphology observation (Fig. 1) further confirmed that fines with smaller particle size were more likely to cover the carrier surface.

All the mixtures were homogeneous with recovery rate over 90%, and RSD% <5% (Table 1). No difference in uniformity between different fine lactose powder formulations was found.

3.2. Influence of fine lactose size on rheological properties

Our previous studies have confirmed that DPI formulations' performance is closely related to the powder properties [25]. Therefore, influence of lactose fines size on DPI powders rheological properties was further explored.

First of all, flowability of the mixture was characterized using BFE value as representative. BFE measures the powders flow resistance under confined conditions, and a small BFE value normally corresponds to a good flowability. As indicated in Table 2, the magnitude of BFE value was both fine lactose size and fine content dependent, and a significant BFE decrease was observed with the decrease of fine lactose size (in the order of LH300 < LH230 < LH210) and increase of added fines ratio from 3% to 7% ($p < 0.05$), suggesting improved flowability of the mixture. The added fine lactose may function as a lubricant, making a smoother carrier surface [33] and more close to rolling flow. We suggest at the same fine content, the smaller the fine lactose size, the easier it is to be embedded on the irregular sites of the carrier surface, thus leading to better lubricating effect. With the increase of fines particle size, the decreased lubricating effect explained the higher BFE value. Moreover, when the fines ratio increased from 3% to 7%, the extent of BFE value decrease was also fine lactose size dependent, and more significant BFE decrease was observed in finer size mixtures, especially in LH300 and LH230 group, whereas the BFE value only decreased slightly in LH210 group when its content increased from 3% to 7%. This result is consistent with previous findings that LH300 fines had the largest, whilst LH210 fines had the least impact on the powder flowability [34]. Therefore, the smaller the fines size and the higher the fines content in DPI system, the better the powder flowability.

Thereafter, adhesion and cohesion properties of the mixtures were further investigated via measuring a variety of interaction relevant parameters, including AE, AR, permeability, FF and cohesion. AE measures the powders' resistance to flow during fluidization [35]. A greater AE value suggests a stronger interaction between particles in the mixture [36]. As shown in Table 2, when the fine ratio was 3%, the mixtures containing smaller size lactose fines had a higher AE value. No statistical difference in AE value between LH300 and LH 230 groups was found when the fine ratio was increased to 5% and 7%, but they were significantly higher than that of LH 210 group ($p < 0.05$), implying mixtures containing smaller size lactose fines was more cohesive. Since the added fine lactose can be well distributed on the carrier surface, the fines and carrier lactose probably fluidize as a whole under the action of airflow [37,38]. However, smaller fines can be easily embedded in the irregular sites of the carrier, generating a stronger binding force between fines-carrier particles, therefore, more energy is required to destroy such binding force to achieve fluidized state of the powders. The same trend was observed via AR measurement. AR is a derivative parameter of AE, which is related with the sensitivity to airflow. A larger AR value usually indicates the DPI powder is more sensitive to air and can fluidize easily [39]. It is noted that AR decreased gradually as particle size of the fine decrease (Table 2), indicating the increase of inter-particle force. Similarly, the permeability decreased as fines size decrease, while the fines may fill in voids and hollows of the powder bed, leading to stronger interactive force in the powders. The same conclusion can be drawn by analyzing the FF and cohesion value. FF is a dimensionless parameter, the more cohesive the powder, the lower the FF value. As for cohesion parameter, it is the sum of total force [40]. As shown in Table 2, FF decrease and cohesion increase was observed as the fine lactose size decrease, with the extent lactose fines ratio dependent. However, it should be noted that cohesion measured via FT4 is derived from flowability, not direct measurement of inter-particular forces.

3.3. Influence of fine lactose size on aerodynamic properties

All the above results have shown that fine lactose size can influence flowability and particle interaction of the carrier-based mixtures. Furthermore, NGI was used to investigate the influence of fines size on aerodynamic properties and lung deposition of the mixtures.

As shown in Fig. 2, when compared at the same weight ratio, with the increase of fine lactose size, drug deposition at the capsule and the pre-separator increased, with decreased deposition at the 1–3 stages. Increasing the fine ratio from 3% to 7% led to increased drug deposition at the 2–3 stages, especially the LH300 group. These studies indicated

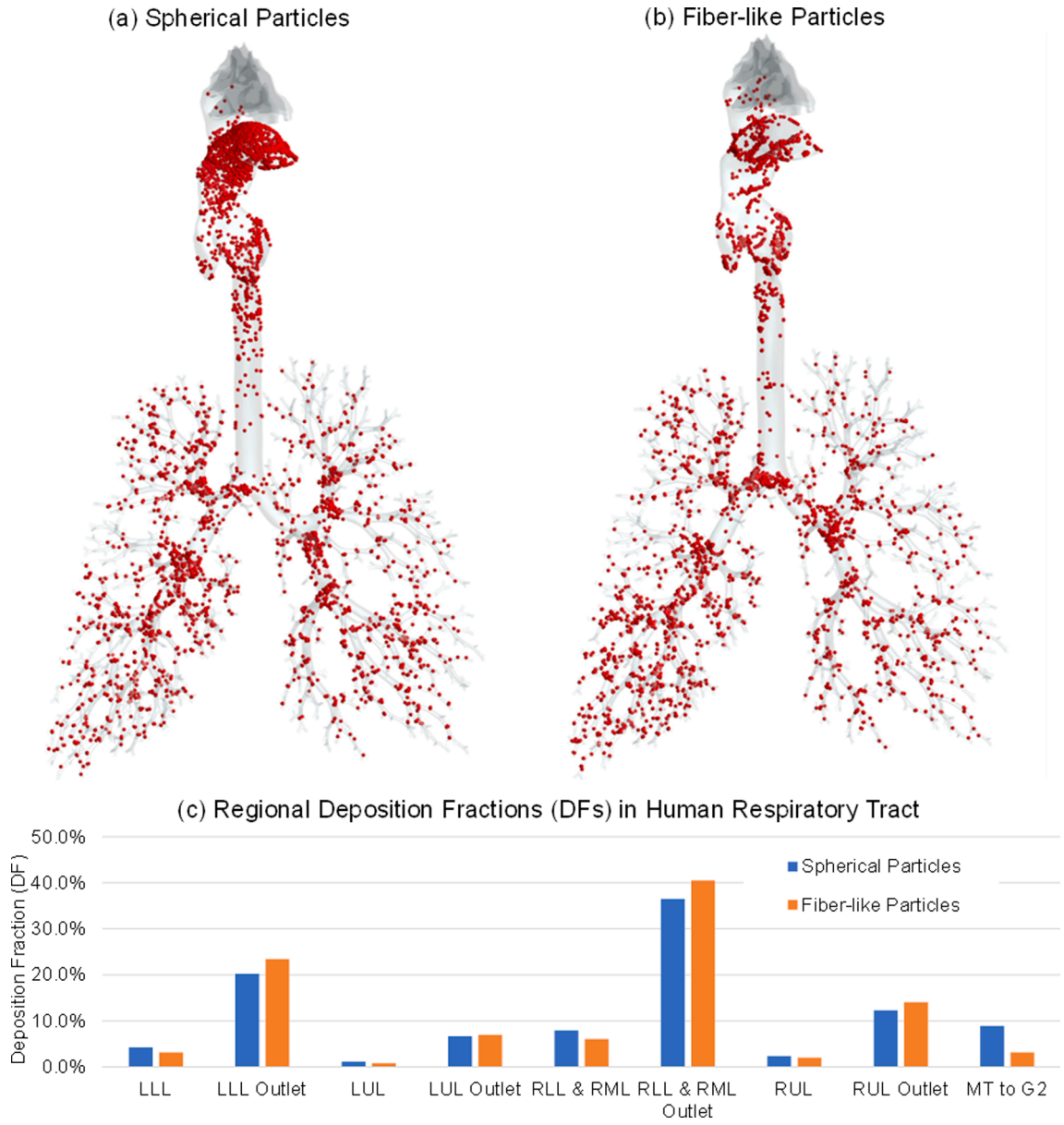

Fig. 6. Comparisons of airway deposition patterns between fibrous particles and spherical particles: (a) Local deposition patterns of spherical particles, (b) Local deposition patterns of fiber-like particles, (c) regional deposition fractions (DFs) in human respiratory tract (LLL: left lower lobe, LUL: left upper lobe, RLL: right lower lobe, RML: right middle lobe, RUL: right upper lobe, MT: mouth-to-throat region).

that the fine lactose with a smaller size can be more beneficial for drug detachment from the carrier surface, with the concrete function its ratio dependent.

Influence of fine lactose size on *in-vitro* performance of the DPI powders was further evaluated by comparing the EF, MMAD and FPF parameters and shown in Fig. 3.

MMAD is a parameter related to the average aerodynamic diameter of drug aerosols. In general, particles smaller than 3 μm will deposit into the alveoli, with 3–5 μm particles into the large bronchi. As presented in Fig. 3, MMAD of the mixtures containing LH300 was significantly larger than that of LH230, LH210 groups when the fines ratio was 7% ($p < 0.05$), suggesting more drug aerosol particles are likely to form larger drug-fine powder aggregates with smaller size fines (LH300). A similar phenomenon has been observed in a previous study indicating that MMAD increased with fines content increase, attributed to the formation of large agglomerates [15]. Moreover, when the powders contain larger amount of fines, tensile strength of the bulk powders can be increased, thus the fines combined with drug particles can be entrained as stronger agglomerates [17].

EF is a parameter related to emptying capability of DPI powders from inhaler and capsules. EF increased with fine lactose size decrease (Fig. 3). EF of the mixtures containing 5% LH300 as fines was significantly higher than the other mixtures ($p < 0.05$), and no significant difference between LH230, and LH210 groups was found. When 7% fines was added, EF of the LH300 and LH230 groups was remarkably higher than the LH210 group ($p < 0.05$). Therefore, a good approach for DPI powders to emit thoroughly from capsule and inhaler could possibly be accomplished by adding fines with smaller size. It is speculated that more drug-fine powder aggregates could be formed in this case, thus, they experience decreased resistance than drug-carrier structures during fluidization, and it is also easier to achieve capsule emptying with better flow properties. However, the results are also strongly dependent on the type of inhaler devices used.

FPF is an important measure of DPI's performance, which describes the *in vitro* pulmonary delivery efficiency. It was noted that FPF had an increasing trend with the decrease of fine lactose size (Fig. 3). When the

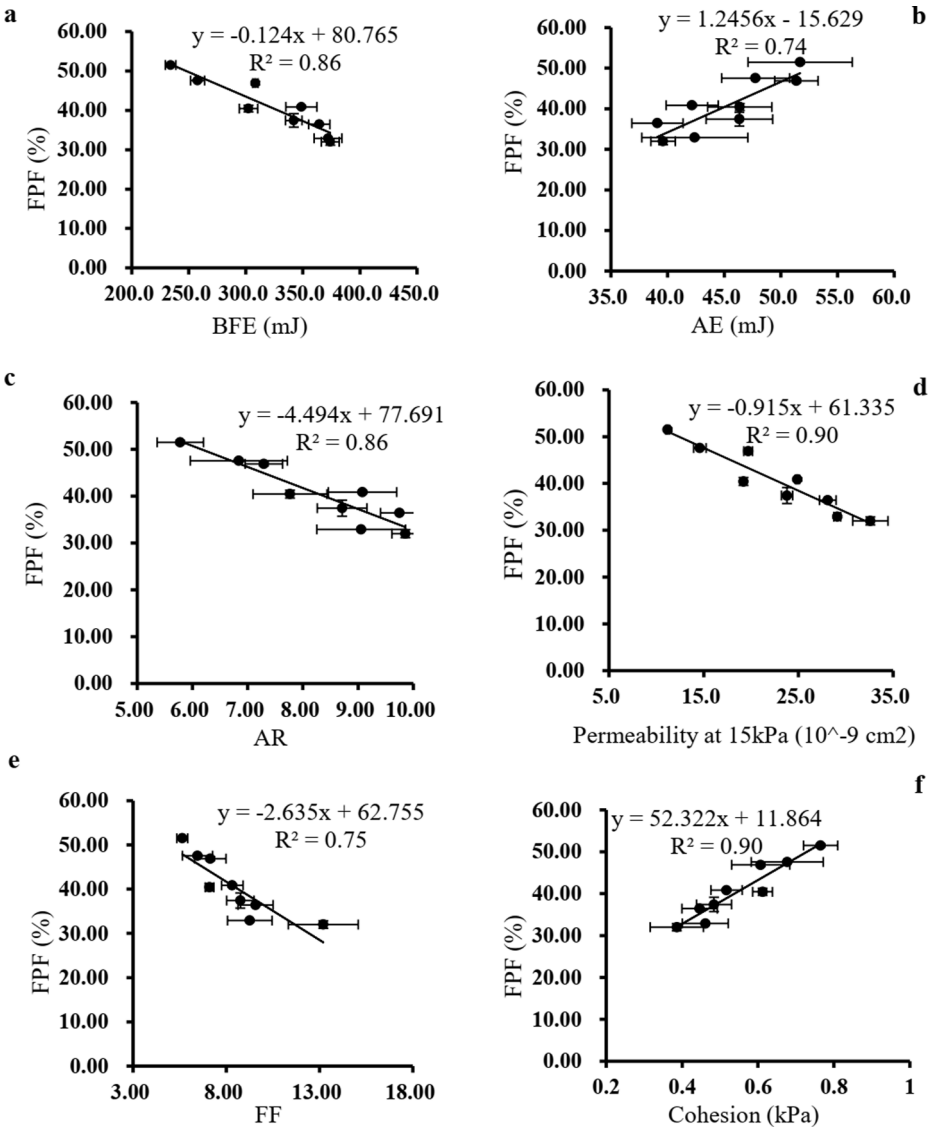

Fig. 7. Correlations between powder properties and FPF (n = 3). (a) BFE–FPF, (b) AE-FPF, (c) AR-FPF,(d) Permeability-FPF, (e)FF-FPF,(f)Cohesion-FPF.

fines content was 3% or 5%, FPF of the LH300 groups was higher than that of the LH230 and LH210 groups ($p < 0.05$). No statistical difference between LH230 and LH210 groups was found ($p > 0.05$). In contrast, when the fine content was further increased to 7%, linearly increased FPF was observed with the decrease of lactose fines size, indicating lactose fines with smaller size is beneficial to improve aerosolization performance of DPI formulations.

Moreover, in order to explain the influence of lactose fine size on DPI's deposition behavior more specifically, we further explored the correlations between FPF and small particle fractions (the small particles here containing the added drug particles), there were, 0–11 μm, 11–21.5 μm, and 21.5–30 μm particles according to the PSD data. As shown in Fig. 4, only the proportion of 0–11 μm fines had a good linear relationship with FPF, indicating 0–11 μm fines has an important influence on FPF. This result is consistent with previous reports, showing fine lactose <10 μm improved salmeterol xinafoate dispersion significantly compared to 10–20 and 20–45 μm size fractions [20,23]. Thereafter, we subdivided the 0–11 μm particles into two size groups, 5.5–11 μm, and <5.5 μm, and as shown in Fig. 4(d and e), similar correlations with FPF were established, implying they have comparable influence on the FPF value and thus they can be taken into consideration as a whole. However, Adi found fines of 5–10 μm fractions resulted in a marked and linear increase in FPF compared to <5 μm fractions, explained by the influence of packing fraction and work of adhesion [23].

The above studies demonstrated that the ratio of 0–11 μm fines can be used as a parameter for FPF prediction. Probably fines in such particle size range can form a larger drug-fines powder aggregates with greater inertia, which present greater inertial force and aerodynamic drag force during inhalation process and then drug particles can be well separated from the carrier surface, thereby more drugs being delivered to the deep lung. However, when the particle size of fine lactose exceeds a certain limit, such as 11 μm in this study, they would serve as a second carrier to carry drug particles, whereas the drug particles might be redistributed from the carrier surface to the added fines, and the increased interactions between drug particles and carriers seemed hardly to improve the aerosolization performance [20,23]. Therefore, the proportion of lactose fines <10 μm is essential to improve the dispersion performance of DPI powders.

3.4. Influence of inhaled particle shape on the distribution of lung deposition

There are multiple particle deposition mechanisms associated with

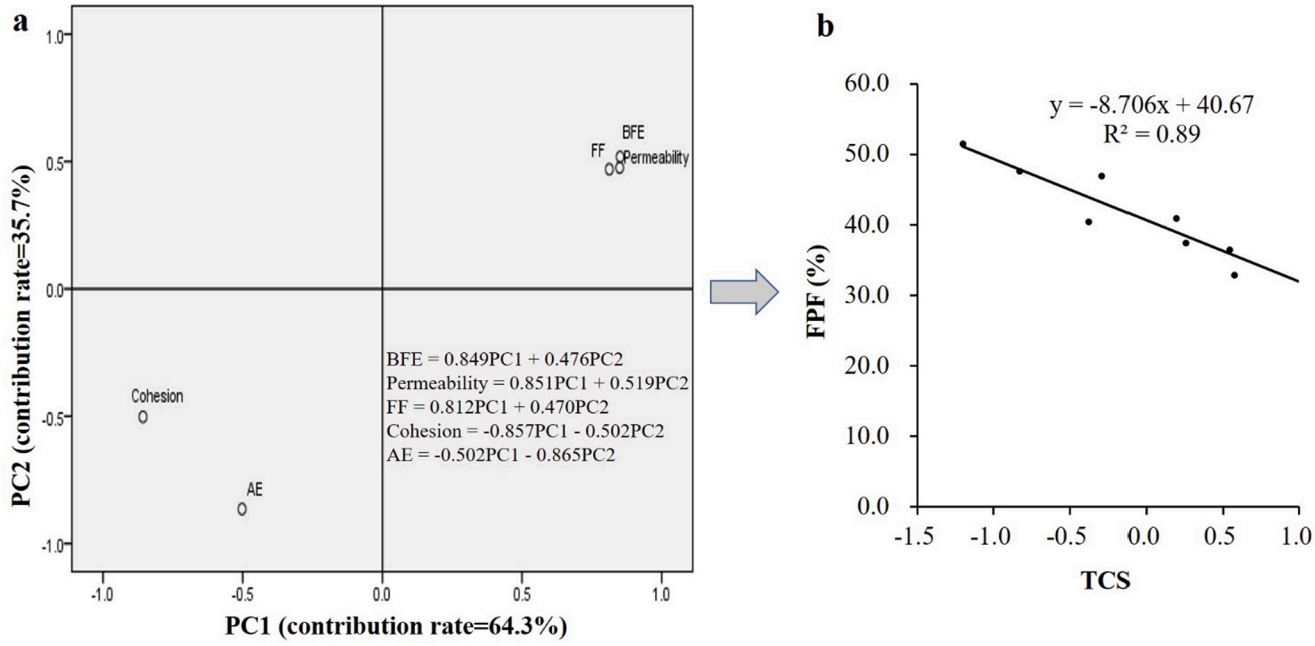

Fig. 8. Component load matrix of rotated principal component matrix from five powder properties (a), and Correlation between TCS and FPF (b).

aerodynamic property when delivered through the pulmonary route, i.e., inertial impaction, gravitational sedimentation, Brownian diffusion, turbulence dispersion, and interception [41]. Previous studies have demonstrated that elongated particles (i.e., fiber-like particles) have significant different aerodynamic characteristics, and can be more easily carried by the pulmonary airflow into deeper lung, with less deposition in the upper airway due to interception compared with spherical particles [27]. Such findings indicate the possibility to utilize particle shape engineering to manufacture elongated aerosolized medication particles to enhance the delivery efficiency to small airways. In addition, some study ascribed to less drug–carrier mechanical interlocking in such shape, further increased drug–carrier detachment during inhalation [42]. Other study further evaluated the effect of fine mannitol shape on DPI's aerosolization performance. It is believed that more elongated fine mannitol particles can reduce drug–carrier or drug–drug contact points [43]. However, above experimental results are all from the perspective of carrier or fine powder shape, rarely drug shape effect on the lung deposition patterns. Moreover, it can be noticed that there can be a great variation in terms of particle size, roughness or crystal structure, all these would affect the judgment of shape influence as discussed previously. As a result, here the CFD-based model was employed to compare drug particle shape on particle lung deposition patterns.

Comparisons of drug particle deposition patterns between spherical particles and elongated particles with aspect ratio equal to 7.5 are shown in Fig. 6(a)–(c). The results indicated that the spherical particles deposition from oral cavity to main trachea was significantly higher than elongated particles with the same aerodynamic diameter distribution (Fig. 5(b)). Furthermore, more spherical particle deposited in the upper respiratory tract would result in lower deep lung deposition than fibrous particles, such difference is due to the fact that the elongated particles are subjected to less airflow resistance in the direction of motion [44]. Specifically, regional deposition fractions (DFs) in Fig. 6(c) shows that increasing the aspect ratio can significantly reduce deposition prior to reaching G6, indicating the enhancement of medication delivery to the lower airways. Specifically, elongated particle depositions in the upper airway (i.e., MT to G2) as well as G3 to G6 (i.e., LLL, LUL, RLL, RML and RUL) are lower than spherical particles. At the same time, more elongated particles can enter the small airways beyond G6. The CFD simulation results are aligned with some studies which also showed needle-shaped crystals have a greater ability to stay airborne in an airflow [10]. Therefore, for the diseases with symptoms in deep lung, drug particles in fiber-like shapes can be delivered more efficiently to such designated lung sites and greatly improve therapeutic effect.

3.5. Correlations between powder properties and lung deposition

DPI formulation is such a complex mixture that pulmonary drug deposition behavior is affected by a variety of variables, which contributes to a great uncertainty for formulation optimization. Therefore, finding the most potential parameters for predicting the *in vitro* aerodynamic performance is an urgent matter to be explored. Our previous studies have investigated the general applicability of powders parameters for predicting FPF based on drug content, drug properties and fine lactose content [21,25,26]. This study here further explored the influence of fine lactose size.

As we can see from Fig. 7(a), BFE and FPF were negatively correlated, indicating good flowability in formulation design is necessary. While powder dispersion via DPIs can be divided into two processes, the first step is powder bed fluidization (reflected in terms of dose emitted from the inhaler). The better the flowability, the easier it is to deliver drug particles from the capsule to the lower respiratory tract [40]. The interaction related parameters, such as AE, AR, Permeability, FF, and Cohesion (Fig. 7(b–f)) all indicated stronger inter-particle forces corresponded to higher FPF, which are relevant to the second step: drug-carrier detachment (evaluated in terms of dose detached from de-aggregation). The increased interactions can be attributed to 0–11 μm fines, which is related to the formation of aggregates and fluidization energy enhancement mechanism.

3.6. Contribution analysis of flowability and interaction

As shown in Fig. 7, both flowability and interaction parameters are related with FPF. However, it is still inconclusive of the utmost importance in determining *in vitro* aerosolization performance. Therefore, in this study, principal component analysis was used to comprehensively analyze BFE, AE, Permeability, FF and Cohesion. From these 5 original parameters, 2 principal components were extracted, which can explain 96.17% variance of the data, suggesting the extracted principal

components can describe most information from the original data.

As shown in Fig. 8(a), contribution rate of PC1 (64.3%) is greater than that of PC2 (35.7%), indicating the degree of data interpretation by PC1 is greater than that of PC2. Furthermore, component load matrix also indicated the degree of correlation between the extracted principal components and the original variables, that is, the influence of each original variable on the principal components. It is demonstrated that PC2 can be defined as interaction index, and PC1 as flowability- interaction balance index. Further, the contribution rate of PC1 was redistributed with the coefficients described in the right of Fig. 8(a), that is, BFE being redistributed as flowability index, the remaining attributed to interaction index. The redistributed results show that the contribution rate of flowability (32.32%) is much lower than that of interaction (67.68%), implying *in vitro* aerosolization performance of DPIs can be more dependent on interaction.

Total component score (TCS) can be obtained from the contribution rate of PC1 and PC2, and correlated negatively with FPF, as shown in Fig. 8(b), indicating a lower TCS is corresponding to a higher FPF. That is, DPI powders with good flowability and meanwhile strong interaction are likely to present an excellent aerodynamic performance.

4. Conclusion

This study explores the influence of fine lactose size on DPIs rheological and aerodynamic properties. Based on the experimental data, more important fines particle size range related with lung deposition is explored. CFD indicates the use of fiber-like particles can also be a potential improvement in oral inhalation. It is believed that, with a better understanding of the influence of lactose or drug fines, it will broaden their application in inhalation for a better therapeutic effect in the future.

- As the particle size of fine lactose decreases, flowability of the mixture is improved, the interaction among particles is increased, and the efficiency of drug deposition in the lung is also improved. Only 0–11 μm fines have a good linear relationship with FPF owing to fluidization energy enhancement and aggregates mechanism. Once exceeding such limit, the fine lactose would act as second carriers, which prevent drug particles detaching from their surface. Moreover, CFD shows elongated drug particles are beneficial to transfer from the upper respiratory tract to the deep lung.
- Dynamic powder properties, such as flowability parameters (BFE), interaction parameters (AE, Permeability, FF and Cohesion), are well correlated with FPF in ternary DPIs based on the influence of fines particle size. Furthermore, PCA results demonstrate interaction parameters are more important to FPF than that of flowability.

Declaration of Competing Interest

The authors declare that they have no known competing financial interests or personal relationships that could have appeared to influence the work reported in this paper.

Acknowledgement

This work is financially supported by the Chunhui Cooperation Research Project of Ministry of Education, China (2019), the National Key R&D Program of China (No. 2020YFE0201700) and Chinese Pharmacopoeia Commission Project (2020Y14, 2021Y17). The research was made possible by funding through the award for project number HR19-106, from the Oklahoma Center for the Advancement of Science and Technology, USA. The use of Ansys software (Ansys Inc., Canonsburg, PA) as part of the Ansys-CBBL academic partnership is also gratefully acknowledged (Dr. Thierry Marchal).

References

[1] Z. Liang, R. Ni, J. Zhou, S. Mao, Recent advances in controlled pulmonary drug delivery, Drug Discov. Today 20 (2015) 380–389.
[2] M.M.A. Elsayed, A.O. Shalash, Modeling the performance of carrier-based dry powder inhalation formulations: Where are we, and how to get there? J. Control. Release 279 (2018) 251–261.
[3] G. Pilcer, N. Wauthoz, K. Amighi, Lactose characteristics and the generation of the aerosol, Adv. Drug. Deliv. Rev. 64 (2012) 233–256.
[4] D.I. Daniher, J. Zhu, Dry powder platform for pulmonary drug delivery, Particuology 6 (2008) 225–238.
[5] S. Mangal, H. Park, R. Nour, N. Shetty, A. Cavallaro, D. Zemlyanov, K. Thalberg, V. Puri, M. Nicholas, A.S. Narang, Q. Zhou, Correlations between surface composition and aerosolization of jet-milled dry powder inhaler formulations with pharmaceutical lubricants, Int. J. Pharm. 568 (2019) 118504.
[6] L. Li, S. Sun, T. Parumasivam, J.A. Denman, T. Gengenbach, P. Tang, S. Mao, H.-K. Chan, l-Leucine as an excipient against moisture on in vitro aerosolization performances of highly hygroscopic spray-dried powders, Eur. J. Pharm. Biopharm. 102 (2016) 132–141.
[7] C. Bosquillon, C. Lombry, V. Préat, R. Vanbever, Influence of formulation excipients and physical characterstics of inhalation dry powders on their aerosolizaton performace, J. Control. Release 70 (2001) 329–339.
[8] Y. Guo, H. Bera, C. Shi, L. Zhang, D. Cun, M. Yang, Pharmaceutical strategies to extend pulmonary exposure of inhaled medicines, Acta Pharm. Sin. B 11 (2021) 2565–2584.
[9] Q. Liu, J. Guan, R. Song, X. Zhang, S. Mao, Physicochemical properties of nanoparticles affecting their fate and the physiological function of pulmonary surfactants, Acta Biomater. 140 (2022) 76–87.
[10] W. Kaialy, On the effects of blending, physicochemical properties, and their interactions on the performance of carrier-based dry powders for inhalation — a review, Adv. Colloid. Interface. Sci. 235 (2016) 70–89.
[11] M. Hoppentocht, P. Hagedoorn, H.W. Frijlink, A.H. de Boer, Technological and practical challenges of dry powder inhalers and formulations, Adv. Drug. Deliv. Rev. 75 (2014) 18–31.
[12] D. El-Sabawi, S. Edge, R. Price, P.M. Young, Continued investigation into the influence of loaded dose on the performance of dry powder inhalers: surface smoothing effects, Drug Dev. Ind. Pharm. 32 (2006) 1135–1138.
[13] P.M. Young, S. Edge, D. Traini, M.D. Jones, R. Price, D. El-Sabawi, C. Urry, C. Smith, The influence of dose on the performance of dry powder inhalation systems, Int. J. Pharm. 296 (2005) 26–33.
[14] A.O. Shalash, M.M.A. Elsayed, A new role of fine excipient materials in carrier-based dry powder inhalation mixtures: effect on deagglomeration of drug particles during mixing revealed, AAPS PharmSciTech (2017).
[15] H. Kinnunen, G. Hebbink, H. Peters, D. Huck, L. Makein, R. Price, Extrinsic lactose fines improve dry powder inhaler formulation performance of a cohesive batch of budesonide via agglomerate formation and consequential co-deposition, Int. J. Pharm. 478 (2015) 53–59.
[16] M.D. Louey, P.J. Stewart, Particle interactions involved in aerosol dispersion of ternary interactive mixtures, Pharm. Res. 19 (2002) 1524–1531.
[17] J. Shur, H. Harris, M.D. Jones, J.S. Kaerger, R. Price, The role of fines in the modification of the fluidization and dispersion mechanism within dry powder inhaler formulations, Pharm. Res. 25 (2008) 1931–1940.
[18] B.H.J. Dickhoff, A.H. de Boer, D. Lambregts, H.W. Frijlink, The effect of carrier surface treatment on drug particle detachment from crystalline carriers in adhesive mixtures for inhalation, Int. J. Pharm. 327 (2006) 17–25.
[19] F. Grasmeijer, A.J. Lexmond, M. van den Noort, P. Hagedoorn, A.J. Hickey, H. W. Frijlink, A.H. de Boer, New mechanisms to explain the effects of added lactose fines on the dispersion performance of adhesive mixtures for inhalation, PLoS ONE 9 (2014).
[20] H. Adi, I. Larson, H. Chiou, P. Young, D. Traini, P. Stewart, Agglomerate strength and dispersion of salmeterol Xinafoate from powder mixtures for inhalation, Pharm. Res. 23 (2007) 2556–2565.
[21] Y. Sun, L. Qin, J. Li, J. Su, S. Mao, Elucidating the effect of fine lactose ratio on the rheological properties and aerodynamic behavior of dry powder for inhalation, AAPS J. 23 (2021).
[22] E. Guenette, A. Barrett, D. Kraus, R. Brody, L. Harding, G. Magee, Understanding the effect of lactose particle size on the properties of DPI formulations using experimental design, Int. J. Pharm. 380 (2009) 80–88.
[23] A. Handoko, L. Ian, S.J. Peter, Influence of the polydispersity of the added fine lactose on the dispersion of salmeterol xinafoate from mixtures for inhalation, Eur. J. Pharm. Sci. 36 (2009) 265–274.
[24] Q.T. Zhou, B. Armstrong, I. Larson, P.J. Stewart, D.A.V. Morton, Understanding the influence of powder flowability, fluidization and de-agglomeration characteristics on the aerosolization of pharmaceutical model powders, Eur. J. Pharm. Sci. 40 (2010) 412–421.
[25] Y. Sun, L. Qin, C. Liu, J. Su, X. Zhang, D. Yu, C. Guo, H. Lu, L. Li, W. Xiong, S. Mao, Exploring the influence of drug content on DPI powder properties and potential prediction of pulmonary drug deposition, Int. J. Pharm. 575 (2020) 119000.
[26] Y. Sun, Z. Cui, Y. Sun, L. Qin, X. Zhang, Q. Liu, X. Shen, D. Yu, S. Mao, Exploring the potential influence of drug charge on downstream deposition behaviour of DPI powders, Int. J. Pharm. 588 (2020) 119798.
[27] Y. Feng, C. Kleinstreuer, Analysis of non-spherical particle transport in complex internal shear flows, Phys. Fluids 25 (2013) 091904.
[28] Y. Feng, J. Zhao, H. Hayati, T. Sperry, H. Yi, Tutorial: understanding the transport, deposition, and translocation of particles in human respiratory systems using

computational fluid-particle dynamics and physiologically based toxicokinetic models, J. Aerosol. Sci. 151, 105672.
[29] J. Zhao, Y. Feng, K. Koshiyama, H. Wu, Prediction of airway deformation effect on pulmonary air-particle dynamics: a numerical study, Phys. Fluids 33 (2021) 101906.
[30] J.F. Zhao, Y.C. Fromen, Glottis motion effects on the inhaled particle transport and deposition in a subject-specific mouth-to-trachea model: an CFPD study, Comput. Biol. Med. 116 (2020).
[31] H. Hayati, Y. Feng, M. Hinsdale, Inter-species variabilities of droplet transport, size change, and deposition in human and rat respiratory systems: an in silico study, J. Aerosol. Sci. 105761 (2021).
[32] J.F. Zhao, Y. Hjaghnegahdar, A. Sarkar, S.R. Bharadwaj, Numerical investigation of particle shape and actuation flow rate effects on lactose carrier delivery efficiency through a dry powder inhaler (DPI) using CFD-DEM, in: 2020 Virtual AIChE Annual Meeting, 2020.
[33] J. Rudén, G. Frenning, T. Bramer, K. Thalberg, G. Alderborn, Relationships between surface coverage ratio and powder mechanics of binary adhesive mixtures for dry powder inhalers, Int. J. Pharm. 541 (2018) 143–156.
[34] H. Kinnunen, G. Hebbink, H. Peters, J. Shur, R. Price, An investigation into the effect of fine lactose particles on the fluidization behaviour and aerosolization performance of carrier-based dry powder inhaler formulations, AAPS Pharmscitech. 15 (2014) 898–909.
[35] K. Almansour, I.M. Alfagih, A.O. Shalash, K. Brockbank, R. Ali, T. Freeman, M.M. A. Elsayed, Insights into the potential of rheological measurements in development of dry powder inhalation formulations, Int. J. Pharm. 614 (2022) 121407.
[36] X. Zhang, Z. Zhao, Y. Cui, F. Liu, Z. Huang, Y. Huang, R. Zhang, T. Freeman, X. Lu, X. Pan, W. Tan, C. Wu, Effect of powder properties on the aerosolization performance of nanoporous mannitol particles as dry powder inhalation carriers, Powder Technol. 358 (2019) 46–54.
[37] M. Hertel, E. Schwarz, M. Kobler, S. Hauptstein, H. Steckel, R. Scherließ, Powder flow analysis: a simple method to indicate the ideal amount of lactose fines in dry powder inhaler formulations, Int. J. Pharm. 535 (2018) 59–67.
[38] E. Cordts, H. Steckel, Capabilities and limitations of using powder rheology and permeability to predict dry powder inhaler performance, Eur. J. Pharm. Biopharm. 82 (2012) 417–423.
[39] H.-J. Lee, H.-G. Lee, Y.-B. Kwon, J.-Y. Kim, Y.-S. Rhee, J. Chon, E.-S. Park, D.-W. Kim, C.-W. Park, The role of lactose carrier on the powder behavior and aerodynamic performance of bosentan microparticles for dry powder inhalation, Eur. J. Pharm. Sci. 117 (2018) 279–289.
[40] E. Faulhammer, V. Wahl, S. Zellnitz, J.G. Khinast, A. Paudel, Carrier-based dry powder inhalation: Impact of carrier modification on capsule filling processability and in vitro aerodynamic performance, Int. J. Pharm. 491 (2015) 231–242.
[41] C. Darquenne, Deposition mechanisms, J. Aerosol. Med. Pulmon. Drug Deliv. 33 (2020) 181–185.
[42] W. Kaialy, A. Alhalaweh, S.P. Velaga, A. Nokhodchi, Effect of carrier particle shape on dry powder inhaler performance, Int. J. Pharm. 421 (2011) 12–23.
[43] W. Kaialy, A. Nokhodchi, Engineered mannitol ternary additives improve dispersion of lactose-salbutamol sulphate dry powder inhalations, AAPS J. 15 (2013) 728–743.
[44] Y. Feng, T. Marchal, T. Sperry, H. Yi, Influence of wind and relative humidity on the social distancing effectiveness to prevent COVID-19 airborne transmission: a numerical study, J. Aerosol. Sci. 105585 (2020).